

High β_{pol} discharges at the Greenwald density with mainly non-inductively driven current in ASDEX Upgrade

J. Hobirk, R. C. Wolf, O. Gruber, A. Gude, S. Günter, B. Kurzan, M. Maraschek, P. J. McCarthy*, H. Meister, A. G. Peeters, G. V. Pereverzev, J. Stober, and ASDEX Upgrade Team

Max-Planck-Institut für Plasmaphysik, EURATOM Association,
Boltzmannstr. 2, 85748 Garching

* Physics Department, University College Cork, Association Euratom-DCU,
Cork, Ireland

For a stationary fusion reactor a possibility to drive the necessary current non-inductively is needed. The discharges presented in this paper combine some useful conditions: the confinement time scales like an H-mode, the density reaches the Greenwald density and the current is driven almost completely non-inductively. The discharge conditions are in many aspects similar to the ones in JT-60U [1, 2] where high poloidal and normalized β has been achieved some years ago. Opposite to this scenario at JT-60U where the density was kept low, the ASDEX Upgrade discharges are nearly automatically at high densities. The discharges combine some features of other advanced scenarios like an internal transport barrier [3, 4] and a monotonic current profile with fishbone activity [5] playing the same role as the sawtooth activity in normal H-modes.

To create a high poloidal β , high neutral beam heating power of $P_{\text{NBI}} = 10\text{MW}$ was injected into a plasma with a low current of $I_P = 400\text{kA}$. The low current together with a toroidal magnetic field of $B_T = 2\text{T}$ corresponds to $q_{95} = 9$. Time traces of the major plasma parameters are shown in fig 1. At $t = 2.6\text{s}$ $\beta_{\text{pol}} = 3$, $\beta_N = 2.7$, and a confinement improvement factor above L-mode ($H_{89\text{P}} = 1.8$), corresponding to $\beta_N \cdot H_{89\text{P}} = 4.8$, have been reached. In the first trace of figure 1 the total plasma current and the NBI heating power are presented. The plasma current decreases from $t = 2.5\text{s}$ onward because the flux in the ohmic transformer is kept constant while it is still required to sustain the 400kA of total plasma current. The heating power is increased in four steps of 2.5MW to a total auxiliary heating power of 10MW at $t = 2.4\text{s}$. In the next part of the figure the line averaged electron density and the Greenwald factor \bar{n}_e/n^{Gw} are shown. The density is increased by gas puffing until 2.4s. Subsequently it is sustained

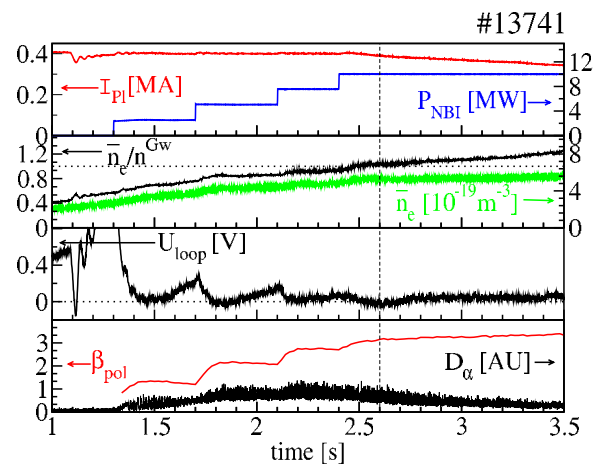


Figure 1: Time traces of the main plasma parameters of a high- β_{pol} discharge. In the upper part the plasma current and the neutral beam heating power, in the second trace the line averaged density and the Greenwald factor are shown, followed by the loop voltage, the D_α trace and the poloidal beta trace at the bottom. The dashed line indicates where a more detailed analysis is done.

subsequently it is sustained

at a constant level by beam fuelling only (natural density). The loop voltage is shown in the next trace. It decreases with each additional heating power finally reaching slightly negative values at about $t = 2.5$ s. After the flux in the ohmic transformer is kept constant the loop voltage increases somewhat and then remains constant at a low positive value. In the bottom trace of fig. 1 the edge D_α emission and the poloidal beta are presented. In the D_α emission the ELM activity can be seen from the first heating step onwards, indicating the H-mode transition. After $t = 2.5$ s the D_α emission decreases and the ELMs become less pronounced. The poloidal beta increases with every step of the NBI power up to $\beta_{\text{pol}} = 3$ at $t = 2.6$ s. Subsequently it still increases, but only because the plasma current is decreasing and not due to a pressure rise. The dashed vertical line in fig. 1 shows the time point where a more detailed data analysis is performed as discussed below.

To show that not only an edge transport barrier in H-mode but also an internal ion transport barrier has developed, in figure 2 the ion temperature profiles from charge exchange spectroscopy (CXRS) of a high β_{pol} discharge (same as in fig. 1) and H-mode discharge are compared. The H-mode ion temperature profile is scaled (by a factor of 0.56) to agree with the value of the high β_{pol} case in the outer region of the plasma. The gradient length of ion temperature profiles in ASDEX Upgrade H-modes [6] is most likely limited by the ion temperature gradient mode [7] (ITG) dominated heat transport, which is associated with a fixed ratio of central to edge ion temperature [8], whereas the temperature profile in the high β_{pol} discharge is more peaked. A clear reduction of the gradient length at $\rho_{\text{tor}} \approx 0.3$ can be seen at $t = 2.6$ s, accompanied by a flattening of the profile in the plasma center, which indicates the formation of an internal transport barrier and corresponds to an increase of the ion temperature peaking factor from $T_i(0)/T_i(\rho_{\text{tor}} = 0.4) = 1.8$ (normal H-mode) to 2.9 in the high- β_{pol} discharges. A detailed analysis of the ITG mode stability is shown in figure 3. In the upper part the radial electric field (E_r) is displayed. The full line represents the total E_r , consisting of the ∇p contribution (dotted) derived from the C^{6+} impurity density and temperature and contributions from the toroidal (dashed-dotted line) and the (calculated) neoclassical poloidal rotation (broken line) [9]. Despite the low E_r , the large gradient of the poloidal rotation leads to a high $\vec{E} \times \vec{B}$ shearing rate as can be seen in the lower part of figure 3, exceeding the linear growth rate of the ITG instability, as derived from the GLF23 model [10], over most of the plasma cross-section. In this sense we assume that the transport barrier is a sign of the suppression of the ITG turbulence.

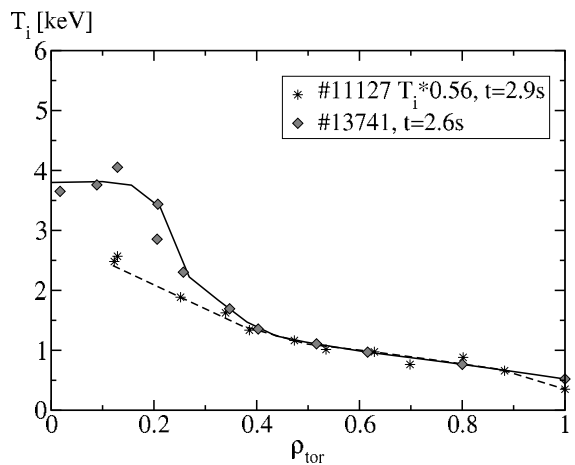


Figure 2: The ion temperature profiles for #13741 at $t = 2.6$ s and for #11127 at $t = 2.9$ s scaled by a factor of 0.56 to be equal in the outer region of the plasma. The symbols represent the actual measured values.

Figure 4 shows the q - and current profiles and its different components as calculated by neoclassical current diffusion and bootstrap current [11] using the ASTRA transport code. For comparison also the profiles inferred from the equilibrium reconstruction based on MSE measurements is presented. Inside $\rho_{\text{tor}} = 0.08$ MSE measurements are not available, indicated by the dotted line. The current diffusion calculation is started at $t = 0.2\text{s}$. At about $t = 1\text{s}$ the loop voltage is spatially almost constant which means that the starting conditions do not influence the resulting current profile strongly. After the heating power ramp the plasma is again in a non-stationary state (mostly because the bootstrap current depends on the current profile itself, providing a kind of feedback loop) until the discharge ends. The contribution of the ohmic current of $I_{\text{OH}} = 25\text{kA}$ is negligible. Main parts are the neutral beam driven current of $I_{\text{NBI}} = 166\text{kA}$, which is broad but peaked towards the plasma center, and the bootstrap current of $I_{\text{BS}} = 200\text{kA}$ with the main contribution in the plasma core. The shape of the total current profile is dominated by the bootstrap current and is in agreement with the one derived from MSE. At the very centre of the plasma the calculations predict strong shear reversal, caused by the drop of the bootstrap current down to zero as the gradients of temperature and density become zero. This feature cannot be resolved by the MSE diagnostic. In agreement with the MSE results the $(1, 1)$ fishbone activity suggests the presence of a $q = 1$ surface. The existence of the strong reversed shear in the plasma core is still unclear because no measurement is available and the standard neoclassical theory breaks down in the plasma core because the trapped particle orbits become large compared to the gradient lengths.

In summary, discharges with high β_{pol} and an internal transport barrier at $\bar{n}_e/n^{\text{Gw}} \approx 1$ have been produced. Transiently, full non-inductive current drive has been demonstrated based on high beam and bootstrap current fractions. Calculations of the ITG mode stability suggest that the favorable transport properties are generated by the neoclassical poloidal plasma rotation which is proportional to the ion temperature gradient. Although $q_{\text{min}} < 1.5$, NTMs do not limit the confinement at 10MW of NBI. Future investigations will concentrate on the enhancement of the bootstrap current by off-axis neutral beam current drive (NBCD). The modification of one of the ASDEX Upgrade neutral beam injectors is near completion with an off-axis current drive capability of up to 250kA. First calculations including the off-axis NBCD show that in addition to the beam current the

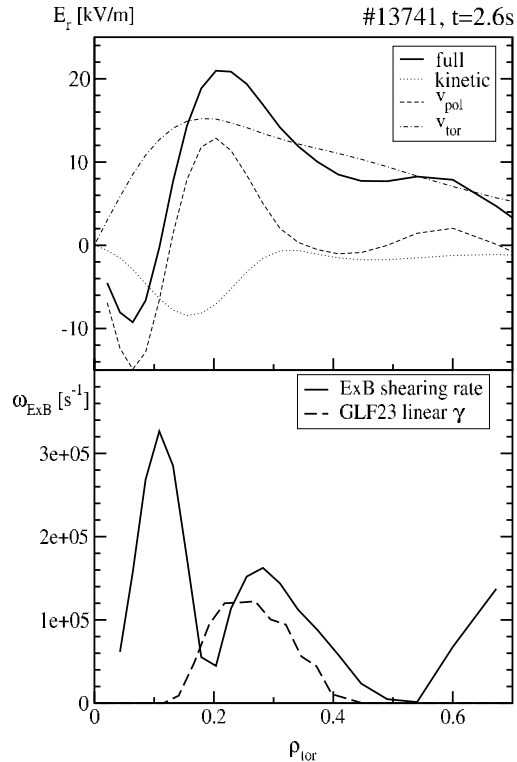


Figure 3: Radial electric field (E_r) profile (full line), consisting of the ∇p part (dotted line) and contributions from toroidal (dashed-dotted line) and neoclassical poloidal rotation (dashed line). In the lower part of the figure the $\vec{E} \times \vec{B}$ shearing rate is compared with the linear growth rate from the GLF23 model (dashed line).

bootstrap current increases due to the effect of the local poloidal magnetic field reduction. This would offer the extension of the operating regime to higher plasma currents while maintaining the improved plasma properties.

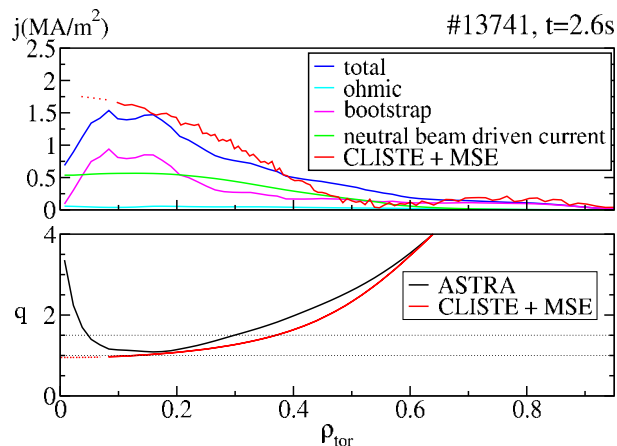


Figure 4: In the upper part the current profile as derived from the transport code ASTRA and from an equilibrium reconstruction by CLISTE using MSE measurements is presented. In the lower part of the figure the corresponding q -profiles are shown.

References

- [1] Y. Kamada *et al.*, Nucl. Fusion **34**, 1605 (1994).
- [2] Y. Koide *et al.*, Phys. Rev. Lett. **72**, 3662 (1994).
- [3] S. Günter *et al.*, Phys. Rev. Lett. **84**, 3097 (2000).
- [4] R. C. Wolf. *et al.*, Physics of Plasmas **7**, 1839 (2000).
- [5] O. Gruber *et al.*, Phys. Rev. Lett. **83**, 1787 (1999).
- [6] A. Stähler *et al.*, Europhysics Conference Abstracts (Proc. 26th Eur. Conf., Maastricht 1999) **23J**, 1437 (1999).
- [7] A. B. Hassam, T. M. Antonsen, J. F. Drake, and P. N. Guzdar, Phys. Fluids B **2**, 1822 (1990).
- [8] A. G. Peeters, Proc 18th IAEA Fusion Energy Conference (Sorento), IAEA-CN-77/EXP5/O6, 2000.
- [9] Y. B. Kim, P. H. Diamond, and R. J. Groebner, Phys. Fluids B **3**, 2050 (1991).
- [10] R. E. Waltz *et al.*, Phys. Plasmas **4**, 2482 (1997).
- [11] W. A. Houlberg, K. C. Shaing, S. P. Hirshman, and M. C. Zarnstorff, Physics of Plasmas **4**, 3230 (1997).